AGU PUBLICATIONS

JGR

Journal of Geophysical Research: Space Physics

RESEARCH ARTICLE
10.1002/2017JA024392

Key Points:
- The patterns of EEJ-induced field and TEC were found to be disrupted significantly before, during, and after the peak SSW
- Substantial influence of lunar tides was observed during the SSW event
- Anomalous depletion in nighttime TEC was observed over low latitudes after the SSW peak

Correspondence to:
S. Yadav,
sneha.yadav84@gmail.com

Citation:
Yadav, S., Pant, T. K., Choudhary, R. K., Vineeth C., Sunda, S., Kumar, K. K., … Mukherjee, S. (2017). Impact of sudden stratospheric warming of 2009 on the equatorial and low-latitude ionosphere of the Indian longitudes: A case study. *Journal of Geophysical Research: Space Physics*, *122*, 10,486–10,501. https://doi.org/10.1002/2017JA024392

Received 23 MAY 2017
Accepted 2 SEP 2017
Accepted article online 11 SEP 2017
Published online 5 OCT 2017

Impact of Sudden Stratospheric Warming of 2009 on the Equatorial and Low-Latitude Ionosphere of the Indian Longitudes: A Case Study

Sneha Yadav[1], Tarun K. Pant[1], R. K. Choudhary[1], C. Vineeth[1], Surendra Sunda[2], K. K. Kumar[1], P. R. Shreedevi[1], and S. Mukherjee[3]

[1]Space Physics Laboratory, VSSC, Thiruvananthapuram, India, [2]Airport Authority of India, Shillong, India, [3]Indian Institute of Geomagnetism, Navi Mumbai, India

Abstract Using the equatorial electrojet (EEJ)-induced surface magnetic field and total electron content (TEC) measurements, we investigated the impact of the sudden stratospheric warming (SSW) of January 2009 on the equatorial electrodynamics and low-latitude ionosphere over the Indian longitudes. Results indicate that the intensity of EEJ and the TEC over low latitudes (extending up to 30°N) exhibit significant perturbations during and after the SSW peak. One of the interesting features is the deviation of EEJ and TEC from the normal quiet time behavior well before the onset of the SSW. This is found to coincide with the beginning of enhanced planetary wave (PW) activity over high latitudes. The substantial amplification of the semidiurnal perturbation after the SSW peak is seen to be coinciding with the onset of new and full moons. The response of TEC to SSW is found to be latitude dependent as the near-equatorial (NE) stations show the semidiurnal perturbation only after the SSW peak. Another notable feature is the presence of reduced ionization in the night sector over the NE and low-latitude regions, appearing as an "ionization hole," well after the SSW peak. The investigation revealed the existence of a quasi 16 day wave in the TEC over low latitudes similar to the one present in the EEJ strength. These results have been discussed in the light of changes in the dynamical background because of enhanced PW activity during SSW, which creates favorable conditions for the amplification of lunar tides, and their subsequent interaction with the lower thermospheric tidal fields.

1. Introduction

The ionosphere is the ionized gas in the Earth's upper atmosphere sandwiched between the neutral atmosphere and the magnetosphere. Consequently, it is not only affected by the solar wind magnetospheric processes but also by the processes occurring in the lower atmosphere. The solar ionizing flux and geomagnetic activity, which are considered as the primary drivers of the ionospheric variability, cannot explain a significant portion of its day-to-day variability. The ionospheric variability, not accounted by these main drivers, is approximately 20% during daytime and 33% during nighttime (Rishbeth & Mendillo, 2001), and these variabilities were reported to reach as high as 200% over low latitudes (Zhao et al., 2008). As a result, understanding and forecasting the day-to-day variability of ionosphere has been a challenging task in spite of the concerted efforts over several years. The situation becomes more complex over low latitudes as the ionosphere therein is not only driven by the processes taking place in the lower atmosphere locally but also by the processes occurring in the high latitudes. The sudden stratospheric warming (SSW), which occurs over high latitudes, is one such process that affects the low-latitude ionosphere through changes in dynamics and energetics.

The SSW is a large-scale meteorological phenomenon over the polar winter hemisphere, generated as a consequence of the interaction of enhanced quasi-stationary planetary waves (PWs) with the polar vortex (Matsuno, 1971). The SSWs are associated with a rapid increase in the polar stratospheric temperature and deceleration (minor warming) and often reversal (major warming) of the high-latitude eastward stratospheric winds. The effect of SSWs is not limited to high-latitude stratosphere alone, rather extending to other altitudes and latitudes. Studies in the past demonstrated a significant cooling in the polar mesosphere and lower thermosphere (MLT) during SSWs (Hoffmann et al., 2007; Liu & Roble, 2002; Manney et al., 2009). The atmosphere over low latitudes also experiences significant variability during the SSW, which is observed in terms of heating of mesosphere (Shepherd et al., 2007; Vineeth, Pant, et al., 2009) and cooling in the low-latitude upper troposphere and lower stratosphere (Fritz & Soules, 1970).

The low-latitude ionosphere also experiences dramatic changes during and after the SSW event (Chau et al., 2012, and references therein). The PWs, which are known to amplify during SSW events, can play a significant role in altering the equatorial *E* and *F* region dynamos which, in turn, influence the distribution of ionization over the entire low-latitude ionosphere by the well-known equatorial ionization anomaly (EIA) process (Appleton, 1946). Many observations have demonstrated the signatures of enhanced semidiurnal perturbations during the SSW events in various ionospheric parameters such as EEJ (Sathishkumar & Sridharan, 2013; Sridharan et al., 2009; Vineeth, Kumar Pant, et al., 2009), vertical drifts (Chau et al., 2010, 2009; Fejer et al., 2010), and total electron content (TEC) (Goncharenko, Chau, et al., 2010; Goncharenko, Coster, et al., 2010; Liu et al., 2011; Sripathi & Bhattacharyya, 2012). It has been observed that the variability of TEC over equator and low latitudes during SSW is latitude dependent. For example, Liu et al. (2011) observed a semidiurnal perturbation in the behavior of TEC over low latitudes, but it was absent over equatorial region in the Asian sector during the SSW event of 2009. This is in contrast with what was reported by Goncharenko, Coster, et al. (2010), who observed semidiurnal perturbation over the equatorial region in the Peruvian sector. Similarly, de Jesus, Batista, de Abreu, et al. (2017) reported the presence of semidiurnal perturbation over low latitudes in the Brazilian sector during the SSW event of 2006. Further, in a study dealing with the longitudinal variability of daytime $E \times B$ drifts during the SSW events of 2003 and 2004, Anderson and Araujo-Pradere (2010) found that the semidiurnal perturbations first appeared over the Peruvian sector and 3 days later over the Philippine sector. Similarly, the significant phase differences in the occurrence of semidiurnal perturbations over Jicamarca (using vertical drift) and Asian (using equatorial electrojet) sectors have also been reported by Fang et al. (2012) during the SSW event of January 2009. Nonetheless, a strong connection between semidiurnal perturbations in the EEJ/vertical drift and the lunar tides during SSWs have also been brought out (Fejer et al., 2010, 2011; Park et al., 2012; Yamazaki et al., 2012). It has been shown that the SSW events provide favorable conditions for the amplification of the lunar tides in the upper atmosphere (Sawada, 1956; Stening et al., 1997). This hypothesis is supported by the results presented by Forbes and Zhang (2012) that demonstrated the amplification of lunar tides during the SSW event of January 2009.

The studies regarding the effect of SSW on the equatorial and low-latitude ionosphere over the Indian longitudes have been limited primarily to equatorial regions dealing with the variation in EEJ current system. Two characteristic features that occur over equatorial and low-latitude ionosphere during SSWs, that is, the presence of counter electrojet (CEJ) and semidiurnal perturbation, have been reported extensively over the Indian region (Patra et al., 2014; Sathishkumar & Sridharan, 2013; Sridharan et al., 2009; Vineeth, Kumar Pant, et al., 2009). On the other hand, Sumod et al. (2012) presented the effects of SSWs on different ionospheric parameters starting from *E* region to *F* region over an equatorial station, Trivandrum. Sripathi and Bhattacharyya (2012) investigated the variability of EEJ and GPS-TEC at several stations in India during the SSW event of 2006. The presence of quasi 16 day wave in several ionospheric parameters, for example, EEJ, TEC, and f_oF_2, have also been reported (Laskar et al., 2014; Patra et al., 2014; Sripathi & Bhattacharyya, 2012). It is worth mentioning here that the above studies deal predominantly with the behavior of daytime ionosphere during and after the SSWs. The studies pertaining to the impact of the modified electrodynamics on the entire low latitudes before and after the onset of SSWs are rather sparse. With regard to the effect of SSW on the low-latitude ionosphere, some of the important questions that need to be answered are as follows: (1) When does the effect of SSW begin over equatorial and low latitudes? (2) What is the effect of changing electrodynamics on the nighttime ionosphere? and (3) What is the latitudinal difference in the behavior of ionosphere during SSWs? The present study is an attempt to address these questions, in addition to providing a comprehensive picture on the response of equatorial and low-latitude ionosphere during the SSW event of January 2009.

2. Database

The primary data set of the present study is the Global Positioning System (GPS)-derived TEC over five different stations across India during the January–February 2009 period. These stations are spread over a latitude region of 10°N to 30°N, representing regions from near equator (NE) to low-mid latitudes. These stations are Agatti (10.8°N, 72.1°E, 2.4°N dip latitude), Bengaluru (12.9°N, 77.6°E, 4.1°N dip latitude), Mumbai (19.0°N, 72.8°E, 10.6°N dip latitude), Bhopal (23.2°N, 77.3°E, 14.3°N dip latitude), and Shimla (31.0°N, 77.0°E, 22.1°N dip latitude). Agatti is very close to the magnetic equator, whereas Bengaluru lies just outside the EEJ zone. On the other hand, Mumbai and Bhopal are located in the vicinity of the EIA crest. During solar minimum, as

in the case of 2009, the EIA crest is expected to be located typically at ~20° geographic north (Yadav et al., 2013). This implies that Shimla is located well beyond the EIA crest and can be called as the low-mid latitude station.

The EEJ intensity during January–February 2009 is obtained from the difference between the horizontal component of the current-induced magnetic field at Tirunelveli (8.73°N, 77.70°E, 0.23°N dip latitude) and Alibag (18.5°N, 72.9°E, 10.33°N dip latitude), which are located on and off the EEJ current region, respectively. This is a well-established method to infer the intensity of the EEJ current (Rastogi & Iyer, 1976). The zonal wind data at 98 km were obtained by using a colocated SKiYMET meteor wind radar over Trivandrum (8.5°N, 77.1°E, 0.5°N). The details of this radar and the method for estimating the neutral winds have been described elsewhere (Hocking et al., 2004). A special transmitting scheme is adopted in the SKiYMET radar operating over Trivandrum to avoid the electrodynamical contamination from EEJ/CEJ and to obtain realistic estimation of the wind variability (Kumar et al., 2009).

The stratospheric parameters like temperature and wind at 10 hPa level (~30 km) between 60°N and 90°N during the January–February 2009 period were obtained from the NASA online data service (http://acdb-ext.gsfc.nasa.gov/Data_services/met/ann_data.html). The amplitudes of PWs of zonal wave numbers 1 (PW1) and 2 (PW2) in geopotential height at 10 hPa, 60°N have also been obtained from the above website. The global stratospheric temperature (at 10 hPa level) were obtained from National Centers for Environmental Prediction/National Center for Atmospheric Research (NCEP/NCAR) (https://www.esrl.noaa.gov/) reanalysis data (Kalnay et al., 1996).

3. Results

Figure 1 presents an overview of different stratospheric parameters at 10 hPa (~30 km) over 60–90°N during January–February 2009. These are (a) stratospheric temperature (ST) (K) between 60° and 90°, (b) zonal wind at 60°N, (c) amplitude of PW1 (Z1), and (d) amplitude of PW2 (Z2) in geopotential height at 10 hPa over 60°N. The ST began to rise abruptly from ~210 K on 15 January, reaching a peak value of ~250 K on 23 January, and gradually decreased afterward attaining the typical quiet time value of ~210 K near the end of February 2009. The PW2 activity began to amplify from ~10 January, that is, much prior to the onset of the SSW event, whereas, the PW1 started to increase from ~20 January. The event is considered as the major warming event as it was associated with the reversal of polar stratospheric zonal wind (polar vortex) and it lasted for more than 3 weeks (Manney et al., 2009). The geomagnetically quiet ($Ap < 20$) and very low solar flux ($F_{10.7} < 80$) conditions during January–February 2009 provide ideal conditions for investigating the ionospheric effects pertaining to the forcing from below during the SSW. The anomalies in different stratospheric parameters during the 2009 SSW event along with the solar and geomagnetic activity have been described in detail by Goncharenko, Chau, et al. (2010). The features of the SSW are only briefly described here in order to put the activities over the polar region, that is, PW activity and ST, in the context of the variations observed over low latitudes as described in the next section.

3.1. Variation in the Equatorial Electrojet

Figure 2 depicts the variation of EEJ-induced magnetic field at surface as a function of (top) day of year (DOY), and (bottom) local time and DOY, during the January–February period. The phases of new and full moon periods are indicated by the open and solid circles, respectively. The red arrow marks the time of SSW peak temperature. It is evident from the figure that in early January, that is, well before the SSW event (~DOY 2 to 10), the diurnal peak in EEJ appeared at ~13–14 LT. A slight shift in the peak of EEJ to early in local time was seen from ~DOY 10. It is to be noted here that the enhancement in the PW2 activity also appeared from ~DOY 10 (see Figure 1). The quiet time pattern of EEJ appeared to be perturbed considerably after the ST at polar region began to increase (i.e., after DOY 15) as the diurnal peak shifts to ~1200–1300 LT during this time. With the progression of the days toward the SSW peak, the overall EEJ showed a small shift toward morning, and it is to be noted that the peak intensity of EEJ was observed at ~1000–1200 during the SSW peak. The EEJ intensity showed a significant reduction just prior to the SSW peak for almost 2 days (DOY 20–21). During the SSW peak, that is, at DOY 23–24, the occurrence of CEJ in the afternoon sector (~1400–1600 LT) was observed. However, the CEJ was not observed on the subsequent day (25 January). The most dramatic changes in EEJ, that is, (i) the presence of intense EEJs and (ii) the occurrence of continuous CEJs were observed after the SSW peak (after DOY 27), which incidentally

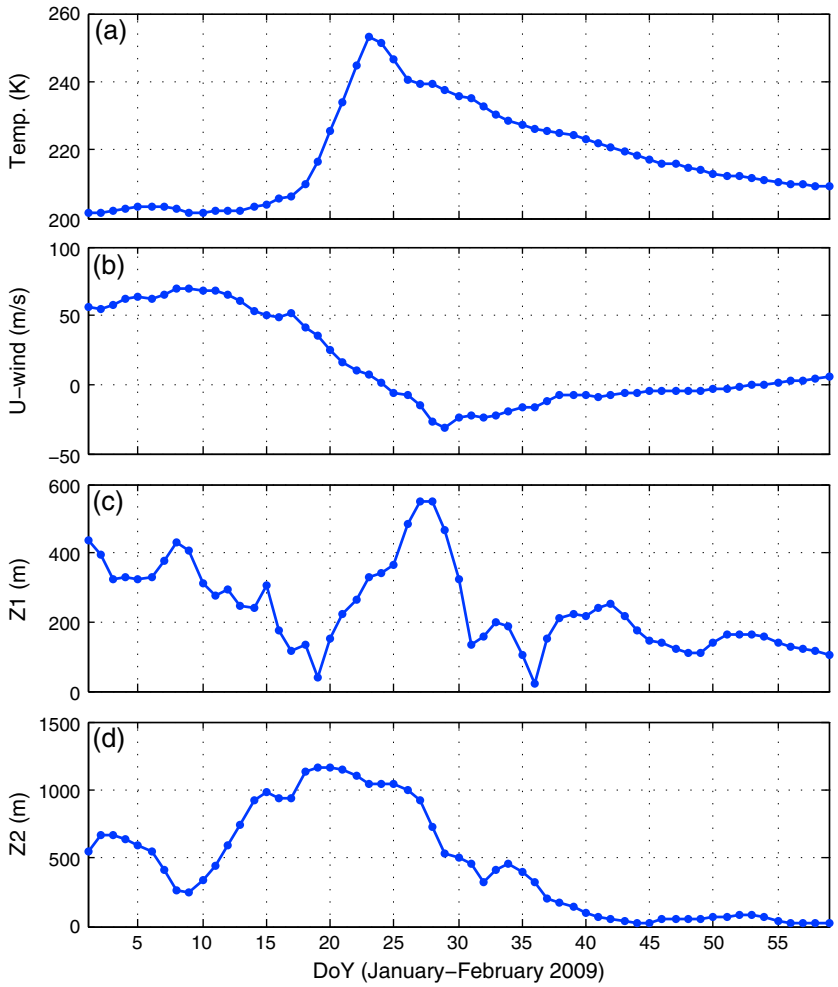

Figure 1. Temporal variation in different stratospheric parameters at 10 hPa (~30 km) over 60–90°N during January–February 2009. (a) Temperature (K) between 60° and 90°, (b) zonal wind at 60°N, (c) amplitude of planetary wave 1 (Z1), and (d) amplitude of planetary wave 2 (Z2) in geopotential height at 10 hPa and 60°N.

coincided with the new moon phase. Interestingly, the intensity of peak EEJ further shifted toward morning and was observed almost 4 h earlier, that is, at ~0900–1000 LT, which systematically shifted to later local time (marked by dashed line) with the phase of the Moon. The intensity of EEJ once again weakened for about 2 days (DOY 35–36) prior to the development of another strong perturbation in the EEJ intensity, which started from DOY 38. It is to be noted that the enhancement in this EEJ intensity coincides with the onset of the full moon. The peak intensity of EEJ again appeared at ~0900–1000 LT, which gradually shifted to later local time (marked by dashed line) with the lunar age possibly marking a recovery to pre-SSW conditions. The presence of strong westward EEJ current (occurrence of CEJ) around the afternoon hours (~1400 LT) was also observed around the new and full moon period, which consistently shifted to later local times as day progressed. Such an enhancement in the EEJ intensity in the prenoon sector with the presence of strong CEJ in the afternoon sector is believed to be due to the influence of semidiurnal tides.

Figure 3 presents a few typical examples of the variation in EEJ intensity (blue solid lines) and zonal wind at 98 km (green dotted lines) for selected days during DOY 1 to 60 as a function of local time. The solid blue and dotted green grid lines depict the zero crossing of the EEJ and zonal wind, respectively. It is observed that the CEJ occurrence was coinciding with the eastward acceleration (deceleration from westward component) of the zonal wind at 98 km. It is to be noted that the days prior to the SSW event (before the stratospheric temperature over the pole started increasing), that is, from 1 to 10, have been considered as normal days. On a

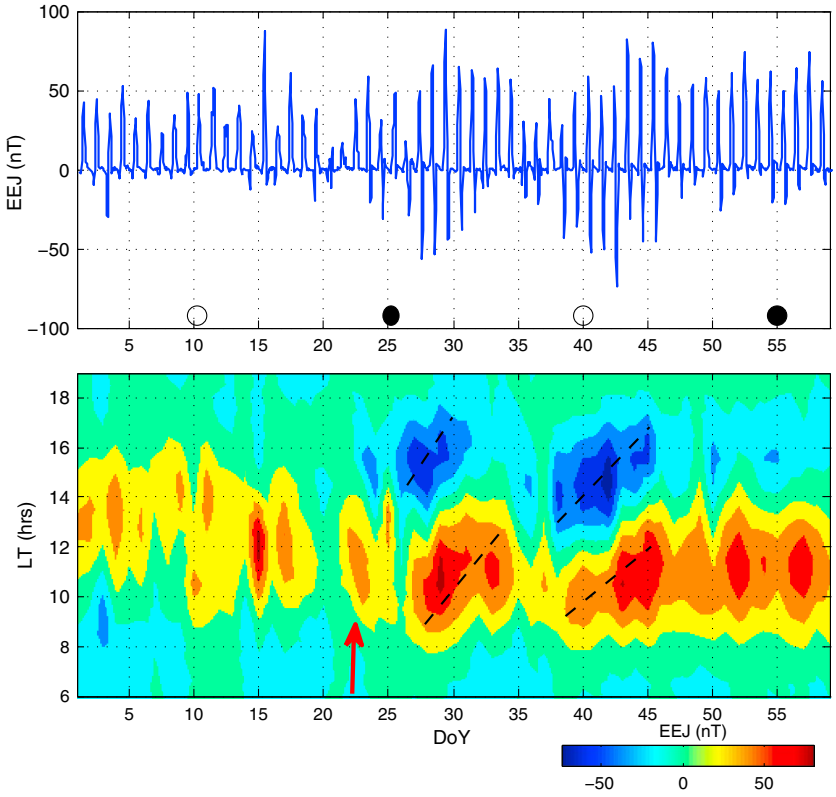

Figure 2. The variation of equatorial electrojet (EEJ) intensity during January–February 2009. (top) Variation of EEJ as a function of day of year (DOY). (bottom) EEJ variation with DOY and local time. The days of new and full moon are indicated by open and solid circles, respectively. Red arrow depicts the time of SSW peak temperature.

normal day (for example DOY 5), the zonal wind at 98 km exhibited an acceleration toward west till 1200 LT and thereafter showed a gradual acceleration toward east. Nonetheless, during the CEJ events, a strong acceleration of zonal wind at 98 km in the eastward direction appeared earlier in local time. It is clear from the figure that such acceleration of zonal wind in the eastward direction (less westward) was observed to be shifted toward morning after the SSW peak (DOY 23). On DOY 25, a steady acceleration of the zonal wind toward eastward direction was observed from ~1200 LT, and followed by this, the CEJ occurred at ~1500 LT. On DOY 30 and 35, the zonal wind at 98 km began to accelerate in the eastward direction from ~ 1200 to 1300 LT and exhibited an eastward excursion at around 1600 LT. The deceleration of zonal wind in the westward direction was seen to occur concurrently with the reversal of the EEJ current at ~1400 LT. Similarly, the zonal wind exhibited an eastward acceleration (less westward) from ~1100 LT on DOY 39, which was found to be coinciding with the reversal of the EEJ current at ~1130 LT. After DOY 39, the eastward acceleration of zonal wind started to shift gradually toward evening. It must be mentioned here that an eastward increase in the zonal wind at 98 km altitude during CEJ events over Trivandrum has already been reported by Vineeth et al. (2012).

3.2. Effect of SSW on the Temporal Variation of TEC Over Low Latitudes

Figure 4 presents the spatiotemporal evolution of TEC as a function of DOY during January–February 2009 over four stations: (a) Bengaluru, (b) Mumbai, (c) Bhopal, and (d) Shimla. Although not shown here, the variations over Agatti and Bengaluru were found to be similar. Therefore, the variations over Bengaluru have only been presented in the figure. In order to show the effect of SSW on TEC, the ST at 10 hPa over 60–90°N latitudes has been plotted in each panel (red curves). In general, the variations in the TEC over low-latitude stations followed the changes in the EEJ intensity. It is observed that the diurnal pattern of TEC over low-latitude stations began to disrupt well before the onset of the peak SSW, that is, from DOY 10 onward. It can be noted from the figure that before the onset of the SSW event (DOY 1–5), the enhanced daytime TEC was generally observed between ~1200 and 1900 LT over Mumbai, whereas, over Bhopal and Shimla, it occurred between

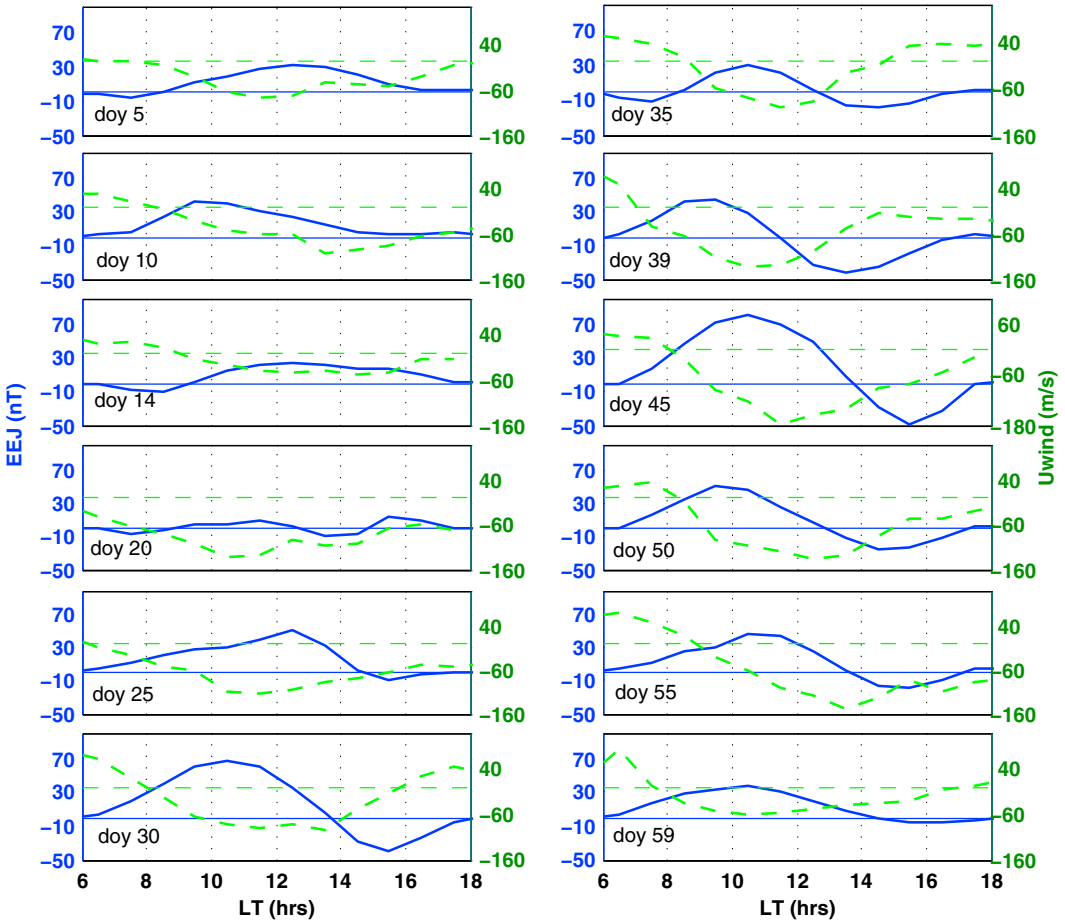

Figure 3. Variation of EEJ (blue solid line) and zonal wind (green dashed line) at 98 km as a function of local time (LT) for different days before and after the SSW event. The solid blue and dotted green grid lines indicate the zero crossing for EEJ and zonal wind, respectively.

~1200 and 1700 LT. On the other hand, the near-equatorial (NE) station (Bengaluru) showed an enhancement in TEC between ~1000 and 2000 LT with no discernible peak. Interestingly, after the SSW peak, the spread in the enhanced TEC over low-latitude stations were observed for a shorter time span. For example, around DOY 35, the enhanced TEC was observed between ~1000 and 1500 LT, ~1200 and 1500 LT, and ~ 0900 and 1700 LT over Mumbai, Bhopal, and Bengaluru, respectively. Nevertheless, such a feature is not present over the low-mid latitude station, Shimla.

The daytime peak TEC values over the low-latitude stations before the onset of the SSW event occurred in the afternoon sector, that is, at ~1500 LT. This daytime peak in TEC appeared to be shifting toward morning as the days progressed. This feature has been highlighted by the white dotted line in the figure. The shift in the daytime peak TEC values toward morning is seen prominently after the peak SSW, that is, during DOY 25–45. In spite of the data gap, these features are also discernible over Shimla, a low-mid latitude station. In contrast to the low-latitude stations, the daytime TEC over the NE station shows a tendency to shift toward morning only after the SSW peak. The observed shifting in the time of maximum TEC toward morning hours, which manifested as a tilted structure in TEC, persisted up to ~DOY 40. The strong enhancement in TEC during ~DOY 27–31 was observed over all the low-latitude stations, while it was absent over Bengaluru, a NE station. As mentioned earlier, the strong enhancement over low latitudes was associated with an intense EEJ during that time period. Another notable feature is that the daytime peak TEC values during ~DOY 27–31 exhibit a shift toward evening, which is marked by the black dotted line in the figure. The similar feature in the TEC over low-latitude stations was also observed during DOY ~38–45. Over the NE station, relatively reduced TEC was observed in the daytime during ~DOY 30–45.

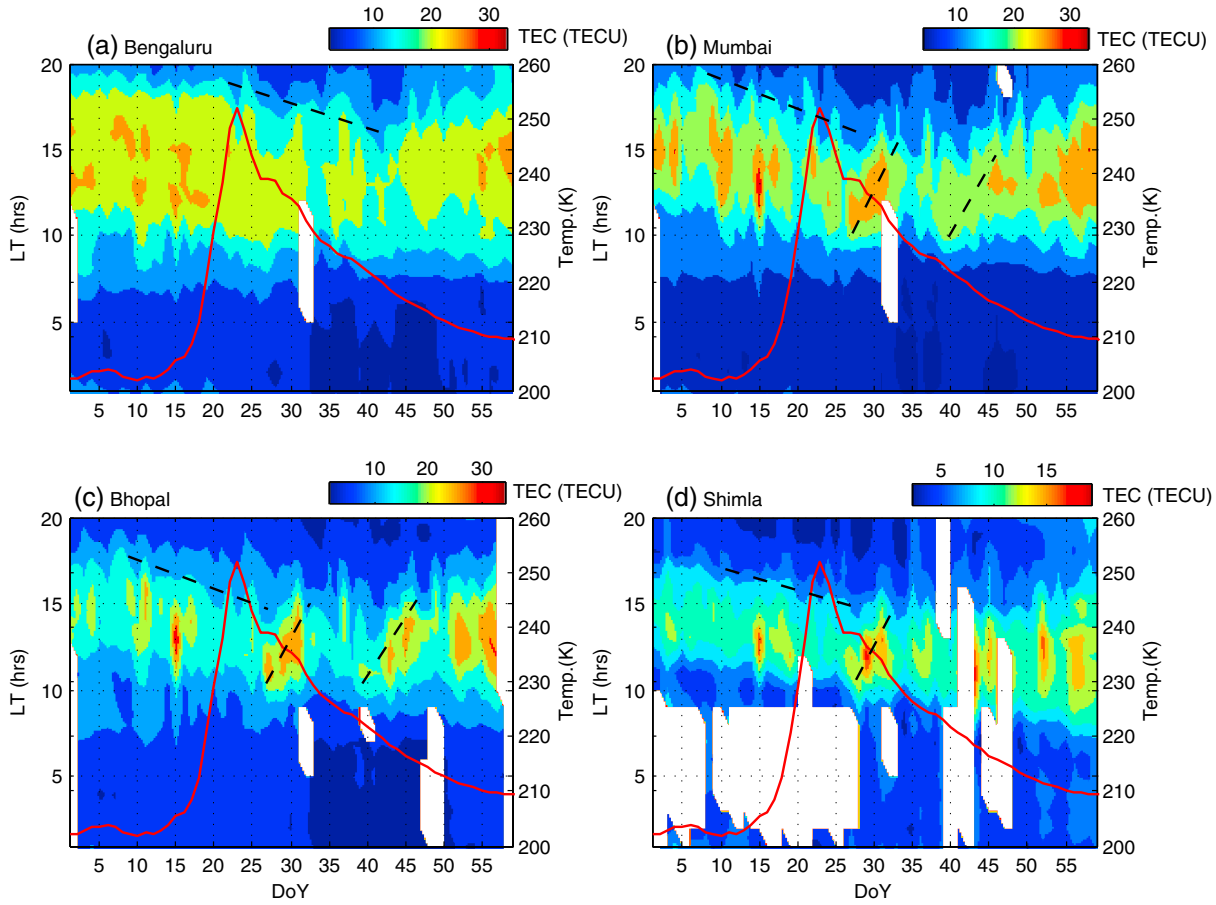

Figure 4. TEC variation as a function local time (LT) and day of year (DOY) during January–February 2009 at (a) Bengaluru, (b) Mumbai, (c) Bhopal, and (d) Shimla. Solid curves represent stratospheric temperature at 10 hPa averaged between 60 and 90°N.

The nighttime ionosphere also displayed an intriguing behavior after the SSW peak. The TEC values during nighttime (~00 to 05 LT) showed a strong reduction during ~DOY 33 to 50. This feature appears conspicuously over Bengaluru and Bhopal but remains less prominent over Mumbai. During normal days (before the onset of the SSW), the TEC over Bhopal and Bengaluru during nighttime (~00–05 LT) varies from ~5 to 10 TECU (total electron content unit, 1 TECU = 10^{16} el m^{-2}). These values were found to be reduced to ~2 to 5 TECU during DOY ~ 33–50. This implies that there is exhibited a more than 50% reduction in the electron density during these days, which can be considered as an appearance of a hole in the ionosphere (referred to as "ionization hole" hereafter). It is to be noted that such an ionization hole was completely absent over the low-mid latitude station, Shimla.

In order to further examine the diurnal changes in TEC over equator and low latitudes, the local time variations of TEC over all the stations on selected days, which span between DOY 15 and 60, representing the days before, during, and after the SSW peak, have been depicted in Figure 5. The solid blue lines in Figure 5 represent the TEC on the selected days, whereas green curves represent the 1 sigma standard deviation of 10 quiet days (i.e., from DOY 1 to 10). In spite of large day-to-day variability, in general, all the stations exhibited the feature of semidiurnal perturbation in TEC. The peak TEC values appear to get shifted toward morning, and there exists a strong reduction in the TEC during the afternoon sector compared to the quiet time reference. The effect is pronounced as the day proceeds, with the maximum effect being observed during ~DOY 30–40 over all the stations. On DOY 60, the daytime TEC again resembles the normal day profile. Unlike the low-latitude stations, the NE stations exhibit the feature of shifting in peak TEC toward morning only after the SSW peak and the effect appeared weak over NE stations as compared to that over low latitudes. The maximum shift in the TEC pattern from the regular pattern is ~0300 h. Liu et al. (2011), for the same SSW event

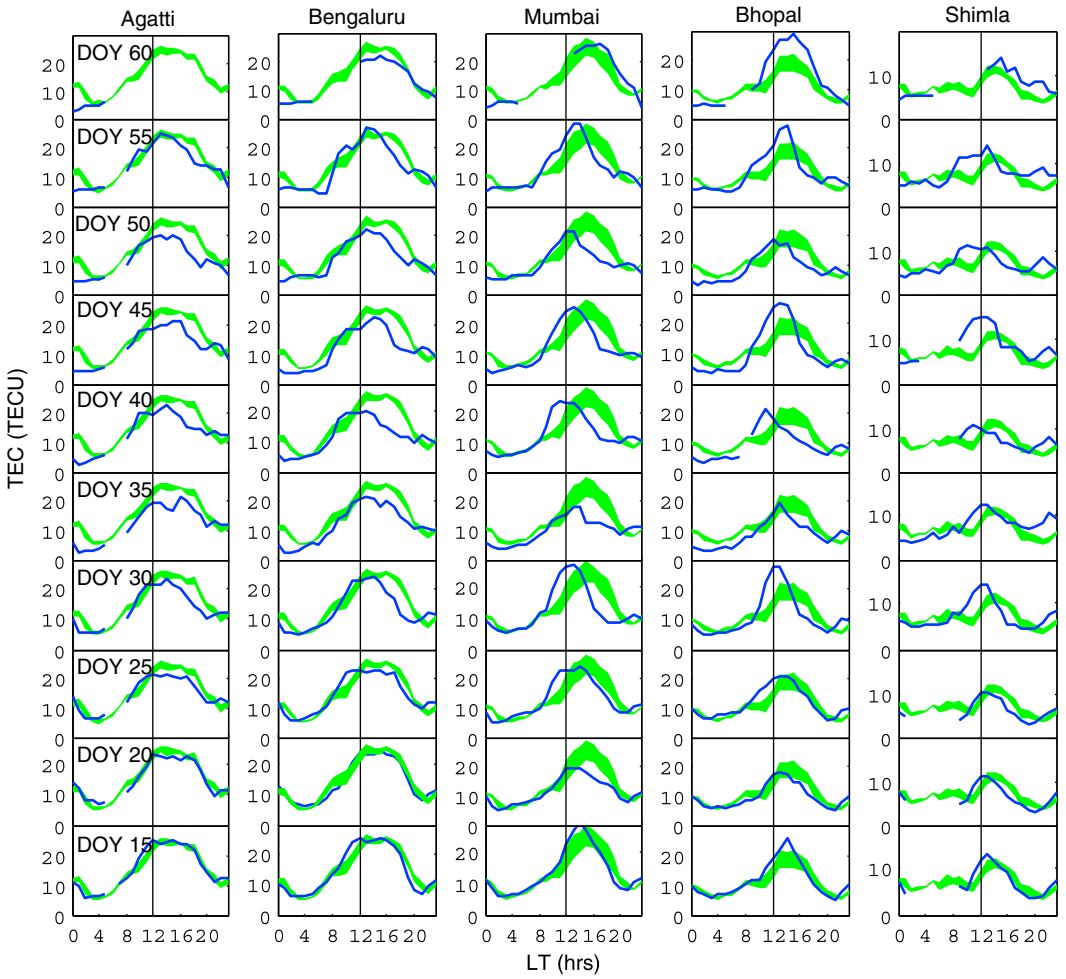

Figure 5. TEC variation during DOY 15–60 plotted at a resolution of 5 days at (first column) Agatti, (second column) Bengaluru, (third column) Mumbai, (fourth column) Bhopal, and (fifth column) Shimla. Green curves indicate the standard deviation of the 10 quiet days at corresponding locations.

of 2009, demonstrated that the TEC variation over EIA crest region exhibited semidiurnal perturbation, and the onset time of the semidiurnal perturbation was on DOY 23 in the Northern Hemisphere and DOY 25 in the Southern Hemisphere over the Asian sector. However, it must be mentioned here that there was a data gap from ~DOY 11–22 over both the EIA crest stations in their study. Similarly, Goncharenko, Chau, et al. (2010) demonstrated the presence of semidiurnal perturbation over equatorial and low latitudes after the SSW peak over the Peruvian sector. Nonetheless, the studies in the past have reported the perturbations in ionospheric electron density after the SSW peak. On the other hand, the present study demonstrates the abnormal behavior of ionosphere over equatorial and low latitudes both before and after the occurrence of the SSW.

In order to study the response of the equatorial and low-latitude ionosphere as a whole to the modified dynamo electric field during the SSW, the peak EEJ and TEC values over the stations considered in this study have been depicted as a function of DOY in Figure 6. The red arrow depicts the time of peak polar ST. In order to examine the correlation between the EEJ and TEC over different stations, the cross-correlation analysis has been performed, and the resulting cross-correlation coefficients have also been marked in the figure. The best correlation is seen over low-latitude stations, Bhopal (R = 0.67) and Mumbai (R = 0.58), as almost all the variations in the EEJ got imprinted in the maximum TEC values over low latitudes. The prominent decrease in EEJ during DOY ~4 to 10 and ~18 to 26 corroborated with a considerable decrease in TEC over the low-latitude stations. The TEC variation at NE stations exhibited a negative correlation with the EEJ.

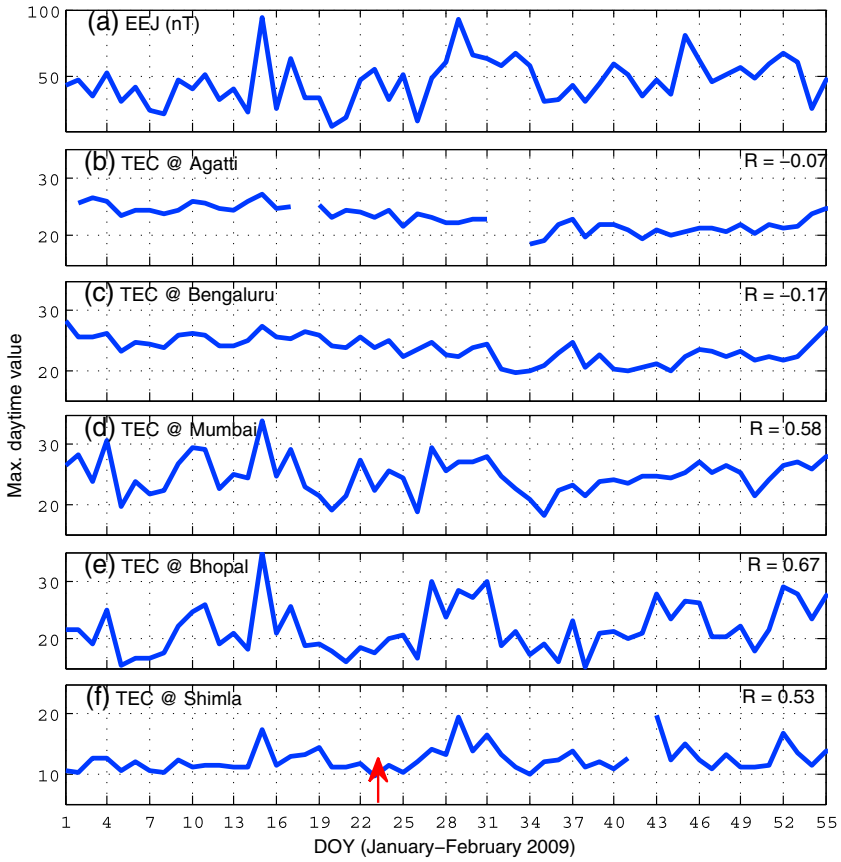

Figure 6. Maximum values of (a) EEJ, and TEC variation over (b) Agatti, (c) Bengaluru, (d) Mumbai, (e) Bhopal, and (f) Shimla during DOY 1–55. The cross-correlation coefficients between maximum EEJ and corresponding stations are also depicted in the figure. Red arrow depicts the time of SSW peak temperature.

However, a fairly well correlation between TEC and the EEJ was observed over the low-mid latitude station, Shimla (R = 0.53), particularly when the maximum EEJ intensity exceeded a value of 50 nT. This implies that, perhaps, the eastward electric field and the subsequent plasma fountain effect played an important role in controlling the electron density over the low-latitude ionosphere extending up to 30°N during the period under investigation.

To investigate the magnitude of semidiurnal perturbation during the morning and afternoon sectors, the values of EEJ, zonal wind, and TEC from 0800 to 1000 LT and 1400 to 1600 LT, respectively, have been averaged out and then subtracted from the corresponding quiet time values. The mean quiet time values are obtained by averaging over 5 days, that is, during 1 to 5 January. Figure 7 depicts the resulting EEJ (Figure 7a) perturbations during the morning (ΔEEJ_m) and afternoon (ΔEEJ_a) sectors. The perturbations in zonal wind during morning (ΔU_m) and afternoon (ΔU_a) sectors is shown in Figure 7b. Similarly, the different panels of Figure 7 also show the calculated ΔTEC_m and ΔTEC_a for Bengaluru (Figure 7c), Mumbai (Figure 7d), Bhopal (Figure 7e), and Shimla (Figure 7f). The positions of full and new moon are depicted in the figure as open and solid circles, respectively. The red arrow depicts the time of peak ST. The ΔEEJ_m and ΔEEJ_a showed the increasing and decreasing trends, respectively, from ~DOY 10, and this behavior seems to increase from DOY 20. The onset of strong semidiurnal perturbation is observed around the SSW peak for all the parameters. The strong amplification in the semidiurnal perturbation, which started close to the onset of the new and full moon periods, can also be easily identified from the figure. The ΔTEC_m and ΔTEC_a over NE station (Bengaluru) show the onset of semidiurnal perturbation only during the onset of the SSW peak. On the other hand, the low-latitude stations, though less pronounced, showed the onset of semidiurnal perturbation immediately after ~DOY 15. It must be mentioned here that such perturbations cannot be delineated over the low-mid latitude station, Shimla, because of the data gap. Nevertheless, the semidiurnal perturbation

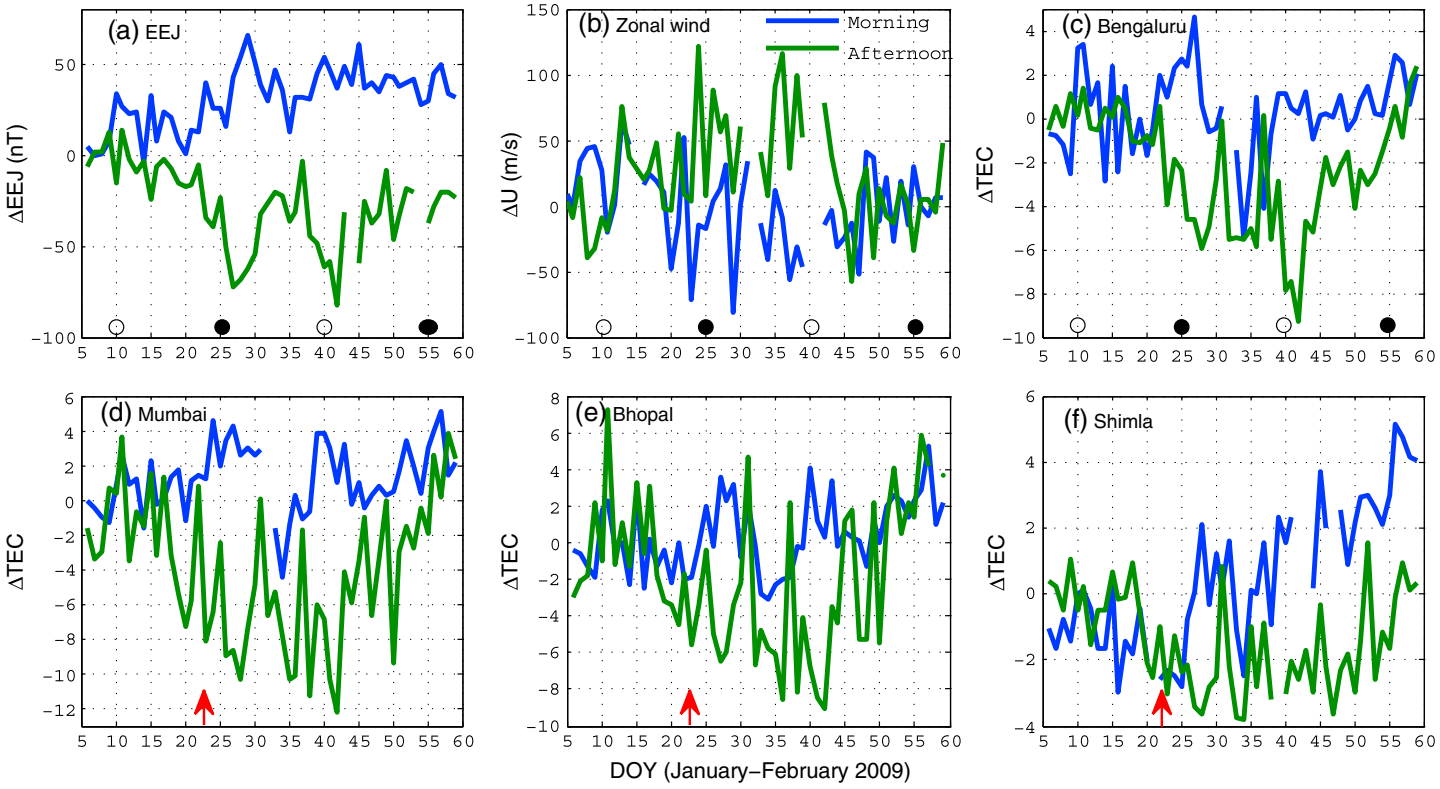

Figure 7. The perturbations (delta variation) around morning (averaged between 0800 and 1000 LT) and afternoon (averaged between 0400 and 1600 LT) sector during DOY 6–59 for (a) EEJ, and TEC over (b) zonal wind, (c) Bengaluru, (d) Mumbai, (e) Bhopal, and (f) Shimla. The delta variations are obtained by subtracting the values on a given day from the quiet time values. Red arrow depicts the time of SSW peak temperature.

increases sharply around the SSW peak over all stations. The most noticeable feature for all the stations is the presence of large semidiurnal perturbations close to the new and full moon periods.

In order to find out the signatures of PWs, which are believed to be interacting with the solar diurnal tides leading to the formation of semidiurnal tides, the fast Fourier transform (FFT) has been applied to the maximum daytime EEJ and TEC values during DOY 3 to 55. Figure 8 presents the amplitude of the normalized spectra hence obtained for EEJ and TEC values over the five stations considered. It is evident from the figure that the dominant period in the EEJ was ~15–17 days. The stations situated inside the EIA zone, that is, Mumbai and Bhopal, show the dominant period of ~13–17 days. However, Shimla, which is normally situated outside the EIA zone, showed the dominant period of ~13–14 days. This suggests that a quasi 16 day (11.2 to 20 days) wave (Salby, 1984) is present over the low-latitude stations during the SSW and absent over NE stations.

4. Discussion

The observed variation in various ionospheric parameters presented in this paper is believed to be caused by PWs, which are known to be enhanced during the SSW event, along with their possible interaction with the lower thermospheric tides. It has been shown that the PWs propagate vertically upward and interact nonlinearly with tides resulting in the enhancement of semidiurnal tides in the lower thermosphere (Hagan & Roble, 2001; Liu & Roble, 2002). The modification in the tides modulate the *E* region electric field via the *E* region dynamo process (Vineeth et al., 2011). The modulated electric field map to the *F* region via equipotential magnetic field lines and the consequent $E \times B$ drift alter the structure of low-latitude ionosphere by changing the EIA phenomenon. The present results also demonstrate the onset of significant semidiurnal perturbation in the EEJ strength and TEC, immediately after the peak SSW. The notable feature is the shift of peak EEJ strength toward earlier local time before the onset of the SSW. The earlier observations on the behavior of ionosphere during SSW deal primarily with the features like semidiurnal perturbations only

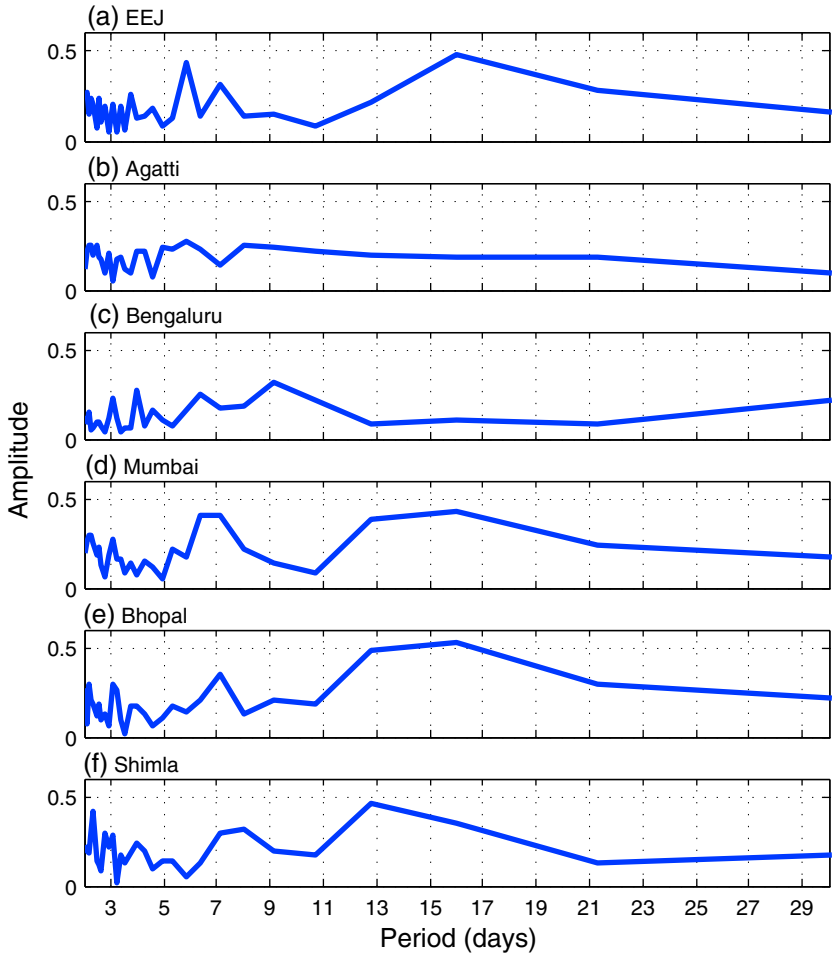

Figure 8. The FFT analysis of maximum daytime values of (a) EEJ, and TEC over (b) Agatti, (c) Bengaluru, (d) Mumbai, (e) Bhopal, and (f) Shimla.

after the SSW peak (Fejer et al., 2010; Goncharenko, Chau, et al., 2010; Goncharenko, Coster, et al., 2010; Liu et al., 2011; Sathishkumar & Sridharan, 2013). However, the present results show the distinct behavior of EEJ and TEC well before the onset of the SSW, which is seen to occur concurrently with the enhanced PW2 activity. It is interesting to note that the increased wave activity prior to the SSW onset has its imprints over the low-latitude ionosphere in spite of the fact that the quasi-stationary PWs that originate from high latitudes remain confined to high and middle latitudes (Pancheva et al., 2009; Pogoreltsev et al., 2007). This presents a classic example of high- to low-latitude coupling as the upward propagating quasi-stationary PWs could change the circulation pattern in the stratosphere and mesosphere over high latitudes (Liu & Roble, 2002) and the modified circulation may affect the low-latitude atmosphere (Sathishkumar et al., 2009). It is a well-established fact that the SSW over high latitudes is accompanied by cooling in the low-latitude upper troposphere and lower stratosphere (Fritz & Soules, 1970; Kodera, 2006) and heating in the tropical mesosphere (Shepherd et al., 2007). The changes in the background energetics and dynamics can cause enhancements in the tidal amplitudes in the lower thermosphere (Hagan et al., 1992; Stening et al., 1997). Figure 9 presents the stratospheric temperature at 10 hPa over the tropics, that is, from 0 to 30°N obtained from NCEP reanalysis data. It is clear from the figure that the stratospheric temperature around the equator shows significant cooling during ~DOY 15 to 48 with maximum cooling at ~DOY 20 to 40 where the temperature drops down to 220 K. It is clear from the above observations that the lower atmosphere over the tropics underwent large-scale changes in the energetics and dynamics.

The present study clearly demonstrates the presence of quasi 16 day PWs (13–17 day periodicity) in both the peak daytime EEJ strength and the TEC over low latitudes extending up to 30°N. The intriguing feature is that

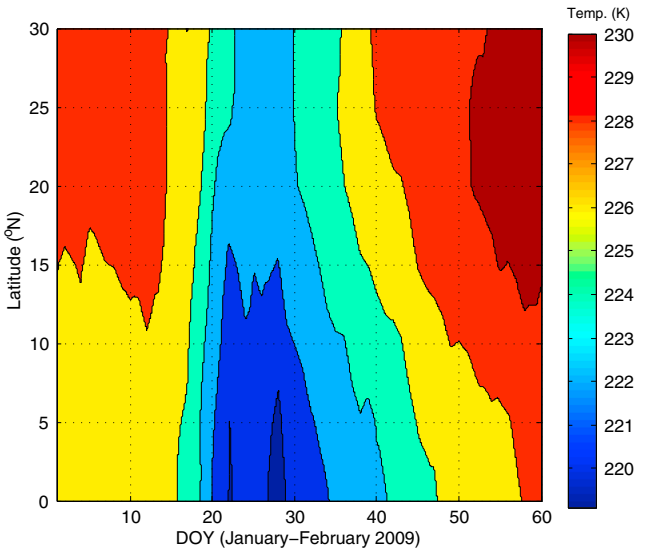

Figure 9. Variation of stratospheric temperature at 10 hPa from 0 to 30°N during DOY 1 to 60 obtained from the NCEP reanalysis data.

this period is absent over the NE stations. The absence of quasi 16 day periodicity around the NE stations suggests that the ionization over NE stations do not get influenced by the EEJ and the consequent fountain effect. The earlier workers also reported the presence of quasi 16 day wave during the SSW events at the low-latitude ionosphere of the Indian zone, which are linked with the changes in the equatorial electric fields (Laskar et al., 2014; Patra et al., 2014; Sripathi & Bhattacharyya, 2012). The presence of quasi 16 day wave during the SSW event of 2013 was also observed over midlatitude ionosphere (Chen et al., 2016). de Jesus, Batista, Fagundes, et al. (2017), during the minor SSW event of 2012, observed a weakening of the quasi 16 day wave in the daily averaged TEC in the Brazilian and African sector with an amplification of the ~2–6 day period in the Brazilian sector. Similarly, periods of ~02–08 days had been reported during a major SSW event of 2006 over the equatorial and low-latitude stations of the Brazilian sector (de Jesus, Batista, de Abreu, et al., 2017). However, the strong contrast between the near-equator (NE) and low-latitude ionosphere, that is, the presence of quasi 16 day wave over low latitudes and its absence over NE station, has not been reported earlier.

The occurrence of the semidiurnal perturbations in the EEJ and TEC during SSW as observed in the present study are consistent with the recent studies performed over different longitude sectors. For instance, Lin et al. (2012) investigated the global response of ionosphere by using the FORMOSAT-3/COSMIC-derived three-dimensional electron density maps and demonstrated the presence of semidiurnal component at EIA crests during the 2009 SSW event. By analyzing the three major SSWs, including the event of 2009, Paes et al. (2014) have demonstrated the presence of semidiurnal perturbations in TEC over the Brazilian sector. The presence of strong semidiurnal perturbation had also been observed over the midlatitude ionosphere during the SSW event of 2013 (Chen et al., 2016). However, the present results highlight the presence of strong semidiurnal perturbations in the zonal wind, EEJ, and TEC after the SSW peak, which amplifies during the onset of new and full moon periods. The main variability in the EEJ during the SSW is the presence of strong CEJs from DOY 26–31 and 38–45 (see Figure 2a). These events are about 12 days apart, which suggests the influence of lunar semimonthly tide (Stening, 1989). Liu et al. (2011) also reported the presence of strong afternoon CEJs over the Southeast Asian sector during DOY 26 to 31 for the SSW event of 2009. It is clear from Figure 6 of Liu et al. (2011) that the strong CEJs during this time had a tendency to shift toward evening. They restricted the analysis to the days around SSW period (i.e., January 2009), and the variability thereafter had not been explored. Similarly, Patra et al. (2014) investigated the variation of EEJ during the 2009 SSW event over the Indian region, but their study also could not highlight the occurrence of two intense CEJ events reported in the present study. The strong semidiurnal perturbation observed in the zonal wind, EEJ, and TEC around new and full moon phases unambiguously suggests the amplification of semidiurnal lunar tide during the 2009 SSW event. Similarly, Xiong et al. (2013) also reported the presence of semidiurnal lunar tide in TEC over the Chinese sector (~120°E) during the 2009 SSW event. It had been demonstrated in the previous studies that the amplitudes of lunar semidiurnal tides are significantly enhanced during the SSW events (Paulino et al., 2012; Sathishkumar & Sridharan, 2013) which, in turn, cause substantial perturbations in the equatorial and low-latitude ionosphere during the SSWs (Fejer et al., 2010; Park et al., 2012; Pedatella et al., 2012; Stening, 2011). Studies have shown that the prevailing atmospheric conditions during the SSWs favor the vertical propagation of lunar tides (Stening et al., 1996). This mechanism is further supported by Forbes and Zhang (2012), who provided the observational evidence to support the hypothesis of changed middle atmosphere circulation during the SSWs facilitating the amplification of the lunar tide in the lower thermosphere. Adding to this, the simulation carried out by Pedatella et al. (2014) revealed notable enhancements in both the migrating semidiurnal solar and lunar tides during the 2009 SSW event. Thus, the SSW event of 2009 is associated with the enhanced levels of lunar semidiurnal wave activity. Therefore, it is clear that such changes in dynamical background will modulate the *E* region electrodynamics which, in turn, will get imprinted on the EEJ intensity and thereby the low-latitude ionosphere, as observed in the present study.

Further, results demonstrate that the response of TEC to the SSW event is latitude dependent and seen prominently over low latitudes as compared to NE regions. The daytime peak TEC was found to be shifted toward morning over low-latitude stations prior to the SSW peak, whereas over NE stations, it appeared only after the SSW peak. Such a shifting in the peak TEC value is believed to be due to the modification of tides (both amplitude and phase) due to its interaction with the enhanced PWs during the SSW. After the SSW peak, the feature of semidiurnal perturbation was observed over both the NE and low-latitude stations. In fact, Goncharenko, Chau, et al. (2010) reported the presence of the semidiurnal perturbations over the dip equator during the same SSW event over the Peruvian sector. However, these results are in contrast with Liu et al. (2011), who could not observe the presence of semidiurnal perturbations in the TEC over Phuket (8.1°N, 98.3°E), a dip equatorial station in the Asian sector.

The results show that the variation seen in equatorial electric field, inferred through the changes in the EEJ-induced magnetic field at the surface, is reflected in the behavior of TEC over the low-latitude ionosphere extending up to 30°N. The influence of fountain effect over 30°N (Shimla) is very unlikely during the low solar activity quiet time conditions. Over the Indian sector, in general, the EIA crest is found to be located in the latitude zone of 15° to 25°N geographic latitudes (5° to 15°N geomagnetic latitudes) during the low solar activity period (Rama Rao et al., 2006). The anomaly crest was observed to extend beyond 25°N only during the geomagnetic disturbances (Dabas et al., 2006; Manju et al., 2009). On the other hand, the present study shows that the region located beyond the EIA crest during solar minimum and quiet geophysical conditions also gets affected significantly by the equatorial fountain effect during special geophysical phenomena like the SSW events.

The occurrence of strong CEJ was observed during, and several days after, the SSW peak. These CEJ events are found to be associated with the eastward acceleration (deceleration from westward component) of zonal wind in the vicinity of EEJ current system. Stening et al. (1996) pointed out that the CEJ events in the Indian sector during northern winter generally occurred during SSW periods and were accompanied by reversals of the eastward wind at a height of 99 km at Saskatoon, Canada (35°S, 107°W). Sridharan et al. (2009) studied the occurrence of CEJs over the Indian longitudes during three major SSW events and showed that SSW events affect the day-to-day variability of CEJ through the enhancement of semidiurnal tides. Vineeth, Kumar Pant, et al. (2009) reported the occurrence of CEJ over Trivandrum (8.5°N, 76.5°E, and dip 0.5°N) with a quasiperiodicity of 16 days associated with SSW events. However, the present study highlights the occurrence of strong semidiurnal perturbations with intense CEJ events during the SSW near new and full moon periods. These strong semidiurnal perturbations during new and full moon were preceded by the presence of ~2 days of reduced EEJ intensities and occurrence of weaker CEJ events. These results are consistent with the findings of Fejer et al. (2010) who had reported the occurrence of semidiurnal perturbations near the new and full moons during the SSW events, which are preceded by ~2 days of reduced EEJ currents. However, the repercussion of this strong semidiurnal perturbation in EEJ and occurrence of intense CEJs during the SSWs on the behavior of nighttime TEC have not been addressed so far. The present study revealed the existence of an anomalous feature during the SSW, which is the appearance of an ionization hole in the nighttime ionosphere over the NE and low-latitude stations. However, this feature is not very clearly seen over the low-latitude station, Mumbai. The presence of this feature of ionization hole over low-latitude stations is believed to be associated with the combined effect of (1) occurrence of intense CEJ in the afternoon sector and (2) shift in the peak daytime EEJ values toward morning. It is known that owing to the presence of strong eastward electric field and the consequent fountain effect, the electron densities around the EIA crest remains higher, which could sustain the ionization even during the postsunset hours. In the present study, the presence of strong westward electric field after ~1200 LT during ~DOY 25 to 45 inhibits the development of EIA during the afternoon hours. Therefore, the ionosphere around the EIA crest region remains less dense as compared to the normal days. It is conjectured that this reduction in electron density around the EIA crest region as compared to normal days would reflect in terms of ionization hole in the nighttime ionosphere where the recombination plays a dominant role. The ionization over Shimla, being not much affected by equatorial electrodynamics under normal conditions, shows the absence of such feature, thereby substantiating the above conjecture. When it comes to the equatorial and NE stations, it is speculated that the prevalence of the westward electric field from afternoon sector brings the ionosphere over the equatorial regions to the lower altitudes of higher recombination. This results in the reduced TEC values over NE stations as compared to the normal days which appeared as an ionization hole. However, the exact reason behind the TEC behavior

over Mumbai, where this effect is not prominently visible, remains inexplicable at this moment and warrants more investigations.

5. Summary

The present paper investigated the impact of the SSW event that occurred during January 2009 on the equatorial electrodynamics (EEJ/CEJ phenomenon) and low-latitude ionosphere using GPS-TEC observations encompassing a region starting from near equator and extending up to 30°N. The results unveil several intriguing aspects on the variability of low-latitude ionosphere during this SSW event. The EEJ and the low-latitude ionosphere experienced strong semidiurnal perturbations during the SSW event. The impact of strong semidiurnal perturbation over the dip equatorial *E* region, characterized by the enhanced EEJ strength in the morning and the occurrence of strong CEJ in the afternoon, were observed in the nighttime ionosphere in terms of the formation of anomalous ionization hole over the NE and low-latitude regions. The effect of semidiurnal perturbation was found to be latitude dependent as the near-equatorial stations showed this feature only after the SSW peak. It is in contrast to low-latitude stations where similar effect was observed much before the SSW peak. The EEJ and TEC over low latitudes showed the signatures of quasi 16 day wave which was found to be absent over NE stations. The strong amplification in the semidiurnal perturbation around the onset of new and full moon periods have been observed in the equatorial and low-latitude ionosphere. These results highlight the impact of enhanced PW activity on the equatorial and low-latitude ionosphere before the onset of SSW along with the influence of lunar tides during the SSW.

Acknowledgments

The TEC data used in the study are part of the GAGAN project, a joint collaboration between Airports Authority of India (AAI) and ISRO. The TEC data could be made available by writing to S. Sunda (s.sunda@gmail.com). The SKiYMET meteor wind radar over Trivandrum could be made available by writing to K. K. Kumar (k_kishorekumar@vssc.gov.in). The stratospheric parameters were obtained from the NASA online data service (http://acdb-ext.gsfc.nasa.gov/Data_services/met/ann_data.html). The global stratospheric temperature data were obtained from NCEP/NCAR reanalysis data (https://www.esrl.noaa.gov/). The *H* component data from two Indian stations (TIR and ABG) which are used to derive EEJ index were obtained from Indian Institute of Geomagnetism, India (http://wdciig.res.in/). S. Y. duly acknowledges the Department of Science and Technology (DST) for the INSPIRE faculty award and Director, Space Physics Laboratory, for hosting the position. S. S. duly acknowledges the AAI for the support and SAC (ISRO) for hosting his position.

References

Anderson, D., & Araujo-Pradere, E. A. (2010). Sudden stratospheric warming event signatures in daytime *ExB* drift velocities in the Peruvian and Philippine longitude sectors for January 2003 and 2004. *Journal of Geophysical Research*, *115*, A00G05. https://doi.org/10.1029/2010JA015337

Appleton, E. V. (1946). Two anomalies in the ionosphere. *Nature*, *157*, 691–693. https://doi.org/10.1038/157691a0

Chau, J. L., Aponte, N. A., Cabassa, E., Sulzer, M. P., Goncharenko, L. P., & Gonzalez, S. A. (2010). Quiet time ionospheric variability over Arecibo during sudden stratospheric warming events. *Journal of Geophysical Research*, *115*, A00G06. https://doi.org/10.1029/2010JA015378

Chau, J. L., Fejer, B. G., & Goncharenko, L. P. (2009). Quiet variability of equatorial $E \times B$ drifts during a sudden stratospheric warming event. *Geophysical Research Letters*, *36*, L05101. https://doi.org/10.1029/2008GL036785

Chau, J. L., Goncharenko, L. P., Fejer, B. G., & Liu, H. L. (2012). Equatorial and low latitude ionospheric effects during sudden stratospheric warming events ionospheric effects during SSW events. *Space Science Reviews*, *168*(1–4), 385–417. https://doi.org/10.1007/s11214-011-9797-5

Chen, G., Wu, C., Zhang, S., Ning, B., Huang, X., Zhong, D., … Huang, L. (2016). Midlatitude ionospheric responses to the 2013 SSW under high solar activity. *Journal Geophysics Research Space Physics*, *121*, 790–803. https://doi.org/10.1002/2015JA021980

Dabas, S., Das, R. M., Vohra, V. K., & Devasia, C. V. (2006). Space weather impact on the equatorial and low latitude *F*-region ionosphere over India. *Annales de Geophysique*, *24*, 97–105.

de Jesus, R., Batista, I. S., de Abreu, A. J., Fagundes, P. R., Venkatesh, K., & Denardini, C. M. (2017). Observed effects in the equatorial and low-latitude ionosphere in the South American and African sectors during the 2012 minor sudden stratospheric warming. *Journal of Atmospheric and Solar - Terrestrial Physics*, *157-158*, 78–89. https://doi.org/10.1016/j.jastp.2017.04.003

de Jesus, R., Batista, I. S., Fagundes, P. R., Venkatesh, K., & de Abreu, A. J. (2017). Ionospheric response to the 2006 sudden stratospheric warming event over the equatorial and low latitudes in the Brazilian sector using GPS observations. *Journal of Atmospheric and Solar - Terrestrial Physics*, *154*, 92–103. https://doi.org/10.1016/j.jastp.2016.12.005

Fang, T.-W., Fuller-Rowell, T., Akmaev, R., Wu, F., Wang, H., & Anderson, D. (2012). Longitudinal variation of ionospheric vertical drifts during the 2009 sudden stratospheric warming. *Journal of Geophysical Research*, *117*, A03324. https://doi.org/10.1029/2011JA017348

Fejer, B. G., Olson, M. E., Chau, J. L., Stolle, C., Luhr, H., Goncharenko, L. P., … Nagatsuma, T. (2010). Lunar-dependent equatorial ionospheric electrodynamic effects during sudden stratospheric warmings. *Journal of Geophysical Research*, *115*, A00G03. https://doi.org/10.1029/2010JA015273

Fejer, B. G., Tracy, B. D., Olson, M. E., & Chau, J. L. (2011). Enhanced lunar semidiurnal equatorial vertical plasma drifts during sudden stratospheric warmings. *Geophysical Research Letters*, *38*, L21104. https://doi.org/10.1029/2011GL049788

Forbes, J. M., & Zhang, X. (2012). Lunar tide amplification during the January, 2009 stratospheric warming event: Observations and theory. *Journal of Geophysical Research*, *117*, A12312. https://doi.org/10.1029/2012JA017963

Fritz, S., & Soules, S. D. (1970). Large-scale temperature changes in the stratosphere observed from Nimbus III. *Journal of the Atmospheric Sciences*, *27*, 1091–1097.

Goncharenko, L. P., Chau, J. L., Liu, H. L., & Coster, A. J. (2010). Unexpected connections between the stratosphere and ionosphere. *Geophysical Research Letters*, *37*, L10101. https://doi.org/10.1029/2010GL043125

Goncharenko, L. P., Coster, A. J., Chau, J. L., & Valladares, C. E. (2010). Impact of sudden stratospheric warmings on equatorial ionization anomaly. *Journal of Geophysical Research*, *115*, A00G07. https://doi.org/10.1029/2010JA015400

Hagan, M., & Roble, R. (2001). Modeling diurnal tidal variability with the National Center for Atmospheric Research thermosphere-ionosphere mesosphere-electrodynamics general circulation model. *Journal of Geophysical Research*, *106*(A11), 24,869–24,882. https://doi.org/10.1029/2001JA000057

Hagan, M. E., Vial, F., & Forbes, J. M. (1992). Variability in the upward propagating semidiurnal tide due to effects of QBO in the lower atmosphere. *Journal of Atmospheric and Terrestrial Physics*, *54*, 1465–1474.

Hocking, W. K., Singer, W., Bremer, J., Mitchell, N. J., Batista, P., Clemesha, B., & Donner, M. (2004). Meteor radar temperatures at multiple sites derived with SKiYMET radars and compared to OH, rocket and lidar measurements. *Journal of Atmospheric and Solar - Terrestrial Physics*, *66*, 585–593.

Hoffmann, P., Singer, W., Keuer, D., Hocking, W. K., Kunze, M., & Murayama, Y. (2007). Latitudinal and longitudinal variability of mesospheric winds and temperatures during stratospheric warming events. *Journal of Atmospheric and Solar - Terrestrial Physics*, *69*, 2355–2366.

Kalnay, E., Kanamitsu, M., Kistler, R., & Cillins, W. (1996). The NCEP/NCAR 40-Year Reanalysis Project. *Bulletin of the American Meteorological Society*, *77*, 437–471.

Kodera, K. (2006). Influence of stratospheric sudden warming on the equatorial troposphere. *Geophysical Research Letters*, *33*, L06804. https://doi.org/10.1029/2005GL024510

Kumar, K. K., Ramkumar, G., & Shelbi, S. T. (2009). Reply to comment by R. Dhanya and S. Gurubaran on 'initial results from SKiYMET meteor radar at Thumba (8.51°N, 77°1E): 1. Comparison of wind measurements with MF spaced antenna radar system'. *Radio Science*, *44*, RS5005. https://doi.org/10.1029/2008RS004123

Laskar, F. I., Pallamraju, D., & Veenadhari, B. (2014). Vertical coupling of atmospheres: Dependence on strength of sudden stratospheric warming and solar activity. *Earth, Planets and Space*, *66*(1), 94. https://doi.org/10.1186/1880-5981-66-94

Lin, C. H., Lin, J. T., Chang, L. C., Liu, J. Y., Chen, C. H., Chen, W. H., … Liu, C. H. (2012). Observations of global ionospheric responses to the 2009 stratospheric sudden warming event by FORMOSAT-3/COSMIC. *Journal of Geophysical Research*, *117*, A06323. https://doi.org/10.1029/2011JA017230

Liu, H.-L., and R. G. Roble (2002), A study of a self-generated stratospheric sudden warming and its mesospheric-lower thermospheric impacts using the coupled TIME-GCM/CCM3, *Journal of Geophysical Research*, *107*(D23), 4695. https://doi.org/10.1029/2001JD001533.

Liu, H., Yamamoto, M., Tulasi Ram, S., Tsugawa, T., Otsuka, Y., Stolle, C., … Nagatsuma, T. (2011). Equatorial electrodynamics and neutral background in the Asian sector during the 2009 stratospheric sudden warming. *Journal of Geophysical Research*, *116*, A08308. https://doi.org/10.1029/2011JA016607

Manju, G., Pant, T. K., Ravindran, S., & Sridharan, R. (2009). On the response of the equatorial and low latitude ionospheric regions in the Indian sector to the large magnetic disturbance of 29 October 2003. *Annales de Geophysique*, *27*, 2539–2544.

Manney, G. L., Schwartz, M. J., Krüger, K., Santee, M. L., Pawson, S., Lee, J. N., … Livesey, N. J. (2009). Aura Microwave Limb Sounder observations of dynamics and transport during the record-breaking 2009 Arctic stratospheric major warming. *Geophysical Research Letters*, *36*, L12815. https://doi.org/10.1029/2009GL038586

Matsuno, T. (1971). A dynamical model of the stratospheric sudden warming. *Journal of the Atmospheric Sciences*, *28*, 1479–1494.

Paes, R. R., Batista, I. S., Candido, C. M. N., Jonah, O. F., & Santos, P. C. P. (2014). Equatorial ionization anomaly variability over the Brazilian region during boreal sudden stratospheric warming events. *Journal Geophysics Research Space Physics*, *119*, 7649–7664. https://doi.org/10.1002/2014JA019968

Pancheva, D., Mukhtarov, P., Andonov, B., Mitchell, N. J., & Forbes, J. M. (2009). Planetary waves observed by TIMED/SABER in coupling the stratosphere–mesosphere–lower thermosphere during the winter of 2003/2004: Part 2—Altitude and latitude planetary wave structure. *Journal of Atmospheric and Solar - Terrestrial Physics*, *71*, 75–87. https://doi.org/10.1016/j.jastp.2008.09.027

Park, J., Lühr, H., Kunze, M., Fejer, B. G., & Min, K. W. (2012). Effect of sudden stratospheric warming on lunar tidal modulation of the equatorial electrojet. *Journal of Geophysical Research*, *117*, A03306. https://doi.org/10.1029/2011JA017351

Patra, A. K., Pavan Chaitanya, P., Sripathi, S., & Alex, S. (2014). Ionospheric variability over Indian low latitude linked with the 2009 sudden stratospheric warming. *Journal Geophysics Research Space Physics*, *119*, 4044–4061. https://doi.org/10.1002/2014JA019847

Paulino, A. R., Batista, P. P., Clemeshaa, B. R., Buriti, R. A., & Schuch, N. (2012). An enhancement of the lunar tide in the MLT region observed in the Brazilian sector during 2006 SSW. *Journal of Atmospheric and Solar - Terrestrial Physics*. https://doi.org/10.1016/j.jastp.2011.12.015

Pedatella, N. M., Liu, H.-L., Richmond, A. D., Maute, A., & Fang, T.-W. (2012). Simulations of solar and lunar tidal variability in the mesosphere and lower thermosphere during sudden stratosphere warmings and their influence on the low-latitude ionosphere. *Journal of Geophysical Research*, *117*, A08326. https://doi.org/10.1029/2012JA017858

Pedatella, N. M., Liu, H.-L., Sassi, F., Lei, J., Chau, J. L., & Zhang, X. (2014). Ionosphere variability during the 2009 SSW: Influence of the lunar semidiurnal tide and mechanisms producing electron density variability. *Journal Geophysics Research Space Physics*, *119*, 3828–3843. https://doi.org/10.1002/2014JA019849

Pogoreltsev, A. I., Vlasov, A. A., Fröhlich, K., & Jacobi, C. (2007). Planetary waves in coupling the lower and upper atmosphere. *Journal of Atmospheric and Solar - Terrestrial Physics*, *69*, 2083–2101. https://doi.org/10.1016/j.jastp.2007.05.014

Rama Rao, P. V. S., Gopi Krishna, S., Niranjan, K., & Prasad, D. S. V. V. D. (2006). Temporal and spatial variations in TEC using simultaneous measurements from the Indian GPS network of receivers during the low solar activity period of 2004–2005. *Annales de Geophysique*, *24*, 3279–3292. https://doi.org/10.5194/angeo-24-3279-2006

Rastogi, R. G., & Iyer, K. N. (1976). Quiet day variation of geomagnetic *H* field at low latitudes. *Journal of Geomagnetism and Geoelectricity*, *28*, 461–478.

Rishbeth, H., & Mendillo, M. (2001). Patterns of F_2-layer variability. *Journal of Atmospheric and Solar - Terrestrial Physics*, *63*, 1661–1680.

Salby, M. L. (1984). Survey of planetary-scale travelling waves: The state of theory and observations. *Reviews of Geophysics*, *22*(2), 209–236. https://doi.org/10.1029/RG022i002p00209

Sathishkumar, S., Sridharan, S., & Jacobi, C. (2009). Dynamical response of low-latitude middle atmosphere to major sudden stratospheric warming events. *Journal of Atmospheric and Solar - Terrestrial Physics*, *71*(8–9), 857–865. https://doi.org/10.1016/j.jastp.2009.04.002

Sathishkumar, S., & Sridharan, S. (2013). Lunar and solar tidal variabilities in mesospheric winds and EEJ strength over Tirunelveli (8.7°N, 77.8°E) during the 2009 major stratospheric warming. *Journal Geophysics Research Space Physics*, *118*, 533–541. https://doi.org/10.1029/2012JA018236

Sawada, R. (1956). The atmospheric lunar tides and the temperature profile in the upper atmosphere. *Geophysical Magazine*, *27*, 636–643.

Shepherd, M. G., Wu, D. L., Fedulina, I. N., Gurubaran, S., Russell, J. M., Mlynczak, M. G., & Shepherd, G. G. (2007). Stratospheric warming effects on the tropical mesospheric temperature field. *Journal of Atmospheric and Solar - Terrestrial Physics*, *69*, 2309–2337.

Stening, R. J. (1989). A diurnal modulation of the lunar tide in the upper atmosphere. *Geophysical Research Letters*, *16*, 307–310. https://doi.org/10.1029/GL016i004p00307

Stening, R. J. (2011). Lunar tide in the equatorial electrojet in relation to stratospheric warmings. *Journal of Geophysical Research*, *116*, A12315. https://doi.org/10.1029/2011JA017047

Stening, R. J., Forbes, J. M., Hagan, M. E., & Richmond, A. D. (1997). Experiments with a lunar atmospheric tidal model. *Journal of Geophysical Research*, *102*, 13, 465–113,471. https://doi.org/10.1029/97JD00778

Stening, R. J., Meek, C. E., & Manson, A. H. (1996). Upper atmosphere wind systems during reverse equatorial electrojet events. *Geophysical Research Letters*, *23*(22), 3243–3246. https://doi.org/10.1029/96GL02611

Sridharan, S., Sathishkumar, S., & Gurubaran, S. (2009). Variabilities of mesospheric tides and equatorial electrojet strength during major stratospheric warming events. *Annales de Geophysique*, *27*, 4125–4130. https://doi.org/10.5194/angeo-27-4125-2009

Sripathi, S., & Bhattacharyya, A. (2012). Quiet time variability of the GPS TEC and EEJ strength over Indian region associated with major sudden stratospheric warming events during 2005/2006. *Journal of Geophysical Research*, *117*, A05305. https://doi.org/10.1029/2011JA017103

Sumod, S. G., Pant, T. K., Jose, L., Hossain, M. M., & Kumar, K. K. (2012). Signatures of sudden stratospheric warming on the equatorial ionosphere-thermosphere system. *Planetary and Space Science*, *63–64*, 49–55. https://doi.org/10.1016/j.pss.2011.08.005

Vineeth, C., Kumar Pant, T., & Sridharan, R. (2009). Equatorial counter electrojets and polar stratospheric sudden warmings: A classical example of high latitude-low latitude coupling? *Annales de Geophysique*, *27*, 3147–3153.

Vineeth, C., Pant, T. K., Kumar, K. K., Jose, L., Sumod, S. G., & Alex, S. (2012). Counter equatorial electrojets: Analysis of the variability in daytime mesopause temperature and winds. *Journal of Atmospheric and Solar - Terrestrial Physics*, *75–76*, 115–121. https://doi.org/10.1016/j.jastp.2011.07.005

Vineeth, C., Pant, T. K., Kumar, K. K., Ramkumar, G., & Sridharan, R. (2009). Signatures of low latitude-high latitude coupling in the tropical MLT region during sudden stratospheric warming. *Geophysical Research Letters*, *36*, L20104. https://doi.org/10.1029/2009GL040375

Vineeth, C., Pant, T. K., Sumod, S. G., Kumar, K. K., Gurubaran, S., & Sridharan, R. (2011). Planetary wave-tidal interactions over the equatorial mesosphere-lower thermosphere region and their possible implications for the equatorial electrojet. *Journal of Geophysical Research*, *116*, A01314. https://doi.org/10.1029/2010JA015895

Xiong, J., Wan, W., Ding, F., Liu, L., Ning, B., & Niu, X. (2013). Coupling between mesosphere and ionosphere over Beijing through semidiurnal tides during the 2009 sudden stratospheric warming. *Journal Geophysics Research Space Physics*, *118*, 2511–2521. https://doi.org/10.1002/jgra.50280

Yadav, S., Dabas, R. S., Das, R. M., Upadhayaya, A. K., & Gwal, A. K. (2013). Temporal and spatial variation of equatorial ionization anomaly by using multi-station ionosonde data for the 19th solar cycle over the Indian region. *Advances in Space Research*, *51*, 1253–1265.

Yamazaki, Y., Richmond, A. D., & Yumoto, K. (2012). Stratospheric warmings and the geomagnetic lunar tide: 1958–2007. *Journal of Geophysical Research*, *117*, A04301. https://doi.org/10.1029/2012JA017514

Zhao, B., Wan, W., Liu, L., Igarashi, K., Nakamura, M., Paxton, L. J., … Ren, Z. (2008). Anomalous enhancement of ionospheric electron content in the Asian-Australian region during a geomagnetically quiet day. *Journal of Geophysical Research*, *113*, A11302. https://doi.org/10.1029/2007JA012987